DETECTION AND CHARACTERIZATION OF CAVITIES UNDER THE AIRFIELD PAVEMENTS BY WAVELET ANALYSIS OF SURFACE WAVES

By:
Nenad Gucunski and Parisa Shokouhi
Department of Civil and Environmental Engineering
Rutgers University
Piscataway, NJ 08854
USA
Phone: (732) 445-4413; Fax: (732) 445-0577
Gucunski@rci.rutgers.edu
ParisaSH@rci.rutgers.edu

PRESENTED FOR THE
2004 FAA WORLDWIDE AIRPORT TECHNOLOGY TRANSFER CONFERENCE
ATLANTIC CITY, NEW JERSEY, USA

APRIL 2004

ABSTRACT

A new approach based on the wavelet analysis of surface seismic waves for detection of cavities under the airfield pavements is proposed. Seismic wave propagation in the pavement system is simulated through a transient response analysis on an axisymmetric finite element model. The airfield pavement system is modeled as a thick pavement layer over a homogeneous half space. Detection and characterization of cavities of different sizes and shapes are considered. The formulation of the continuous wavelet transform (CWT) is briefly discussed, and its advantage over the traditional time and spectral analysis methods is demonstrated through illustrative examples. The response of the pavement at different surface points is presented in the wavelet based time-frequency maps. It is shown that the presence of the anomalies is reflected in the time-frequency map of the surface response. Reflected waves from the boundaries of an anomaly introduce new features of specific time and frequency characteristics in the wavelet time-frequency maps. The characteristics of these features have been used to locate and characterize the cavities.

INTRODUCTION

There are many reported incidents of airfield pavement failures, which have resulted from subsurface voids caused by soil erosion near drain pipes. A number of theses incidents have even led to accidents involving aircraft punching through the pavements (Malvar and Cline [1]). Consequently, nondestructive detection and characterization of cavities under the pavements is an important aspect of airfield pavement evaluation and maintenance. A variety of physical and geophysical techniques are being tested and used for this purpose, such as the Heavy Weight Deflectometer (HWD), Dynamic Cone Penetration (DCP), Ground Penetrating Radar (GPR), gravity gradiometer, magnetic and electromagnetic induction, seismic methods, and imagery analysis. However, none of theses methods is capable of providing a complete, unconditional, solution to the cavity detection problem (Malvar and Cline [1]).

Seismic techniques are usually advantageous where there is a significant rigidity contrast between the sought object and the medium. Therefore, seismic methods are expected to be successful in cavity detection applications. These methods are based on either travel time or spectral analysis of elastic waves generated in a medium due to an impact. Refraction and reflection methods are the most widely used travel-time based seismic techniques. The former usually fails to detect shallow cavities in a stratified medium. The latter is quite successful in detection of deep cavities. However, reflection is difficult to utilize in near-surface cavity detection applications (Cooper and Ballard [2] & Belesky and Hardy [3]). Spectral analysis of surface waves (SASW) is the most widely known spectral based nondestructive seismic technique. It has been primarily used in evaluation of elastic moduli and layer thicknesses of layered systems (Nazarian *et al*. [4]). SASW technique has been used for detection of cavities in several studies (Al-Shayea *et al*. [5], Gucunski *et al*. [6], & Ganji *et al*. [7]). It is important to note that it has been found that the success in anomaly detection in this method is dependant on receiver spacing and location, shear wave velocity, and damping of the surrounding soil medium (Ganji *et al*. [7]).

Surface seismic techniques rely on the analysis of surface response of the medium to an impact source. When a shallow cavity is present, reflected waves from near and far faces of the cavity change the near-surface wave patterns. The study of these changes is responsible for the development of seismic cavity detection techniques. The reflections from cavity faces are of a limited duration. It has been found that (Shokouhi *et al.* [8,9]) they have certain frequency bandwidths. These facts suggest that a joint time-frequency analysis of the response could be more efficient than analyzing it in merely one domain. Wavelet transforms are recently developed mathematical tools, which can extract local and global time and frequency information of a signal efficiently. Representation of the signal in the wavelet based time-frequency plane has been used successfully to develop a procedure for detection and characterization of shallow cavities in a homogeneous medium and under thin pavement layers (Shokouhi *et al.* [8,9]). In this study, the method is applied to the problem of detection and characterization of cavities under thick airport pavements.

Numerical simulations are used in this study to investigate the effects of shallow cavities on surface wave patterns in pavement systems. Four cases of different pavement layer thickness, cavity size, and shape are considered. The basic theory of continuous wavelet transform (CWT) is discussed through a number of illustrative examples. For each case, the response of the pavement at a number of surface points is presented in a wavelet time-frequency plane. The time and frequency signature of the cavity in these maps are studied and used for cavity detection and characterization. The results confirm the findings from the previous numerical and field studies involving the detection of cavities in a homogeneous medium. Therefore, it is concluded that the same procedures can be utilized where a thick pavement layer, such as that of an airfield pavement system, is present. However, the extent of applicability and limitations of this method needs to be evaluated through further laboratory and field experiments.

CONTINUOUS WAVELET TRANSFORM (CWT)

Travel-time based techniques for cavity detection do not provide any information on the change in the frequency content of the response due to a presence of a cavity. On the other hand, spectral analysis based methods rely only on the analysis of the response in the frequency domain. It must be taken into consideration that when using Fourier transforms, the time of the changes in the spectrum cannot be taken into account. Reflections from the cavity boundaries change both the time history and the spectrum of the response recorded at surface points. Therefore, a time-frequency analysis of the surface response can be advantageous over analyzing it in merely one domain.

Wavelet transforms are fairly new mathematical tools, which can be used to present the changing spectrum of a nonstationary signal in a time-frequency plane. A Wavelet transform is a convolution between the signal and a set of analyzing wavelets. Wavelets are the scaled and translated versions of a single function referred to as a mother wavelet. A mother wavelet $\psi(\tau)$ is a well-localized function in both time and frequency domains. A wavelet $\psi_{a,t}(\tau)$ at scale a and time t is obtained through scaling and translating of the mother wavelet function $\psi(\tau)$ according to the following equation

$$\psi_{a,t}(\tau) = \frac{1}{\sqrt{a}} \psi \left(\frac{t-\tau}{a}\right) \tag{1}$$

The continuous wavelet transform (CWT) of a signal $x(\tau)$ using wavelet function $\psi(\tau)$, $W_\psi x$, is defined through the convolution between $x(\tau)$ and analyzing wavelets over a finite range of scales as,

$$W_\psi x_{a,t} = \int_{-\infty}^{\infty} x(\tau) \psi^*_{a,t}(\tau) d\tau \tag{2}$$

where $\psi^*_{a,t}(\tau)$ indicates the complex conjugate of $\psi_{a,t}(\tau)$ .If a signal correlates well with the analyzing wavelet, the wavelet coefficient $W_\psi x_{a,t}$ will be large, otherwise, it will be small. Plotting wavelet coefficients $W_\psi x_{a,t}$ versus scale (which is a reciprocal function of frequency) and time produces a representation of the signal in a time-frequency plane, which is referred to as the signal wavelet time-frequency map.

Having varying bandwidth basis, a wavelet transform can capture both local and global time and frequency information of a signal efficiently. The only constraint imposed on an integrable function for being a wavelet is having a zero mean in the time domain, or a zero DC (direct current) offset in the frequency domain. Therefore, a variety of different types of wavelets have been developed for different analysis purposes. Out of all of the families of wavelets examined, Gaussian real wavelets have shown to be the most appropriate wavelets for this study and thus have been used in the analysis. The Gaussian mother wavelet function and its scaled and translated version are defined by the following equations:

$$\psi(\tau) = -1.786 \tau e^{-\tau^2} \tag{3a}$$

$$\psi_{a,t}(\tau) = \frac{1}{\sqrt{a}} (-1.786) \left(\frac{t-\tau}{a}\right) e^{-\left(\frac{t-\tau}{a}\right)^2} \tag{3b}$$

To illustrate the concept of CWT, a wavelet analysis of a synthetic discrete signal of known characteristics is presented. The signal is obtained from 2048 evenly spaced samples of the following function over the interval $0 < t < 1$ s:

$$x(t) = \sin(35t) e^{-200(t-0.25)^2} + \left(\sin(200t) + \sin(35t)\right) e^{-200(t-0.8)^2} \tag{4}$$

There are two main terms in the signal. The first term contains a sine function of a frequency of about 5.6 Hz. The second term is a combination of two sine functions of approximate frequencies of 5.6 and 31.8 Hz. The signal and its Gaussian CWT time-frequency map are shown in Figure 1. The three components of the signal are clearly distinguishable in the wavelet map. This indicates that the prominent portions of the map are aligned directly below the corresponding portions of the signal. As it is expected, the frequency coordinates of these prominent portions match with the frequency of their corresponding terms in the signal. As it can be clearly seen, the wavelet time-frequency map provides not only the frequency information of the signal but also the time bandwidth of the occurrence of each frequency component.

FINITE ELEMENT MODEL

A typical surface seismic test setup consists of a seismic impact source and a number of receivers on the surface of the medium. Surface seismic techniques are based on the analysis and interpretation of the medium surface response recorded at receiver locations. The seismic test is simulated herein through a transient response analysis on an axisymmetric finite element model of the pavement system. Assuming that the wave propagation occurs in a vertical plane, and no lateral reflected waves are present, the medium can be described as an axisymmetric model with an impact force applied at the origin of the system. Because of a very low strain level induced in the medium, the materials are assumed to be linearly elastic. The shear wave velocities in the soil medium and the pavement layer are considered to be as 150 m/s and 450 m/s respectively. The impact is described by an impulse of a trapezoidal shape of 1-KN amplitude and 5-ms duration. Certain criteria are imposed to ensure that the finite element analysis simulates accurately the surface wave propagation (Ganji *et al*. [7], Zerwer *et al*. [10], & Shokouhi *et al*. [9]). The soil medium is described as a 55-m wide and 35-m deep model discretized by axisymmetric quadratic elements. The smallest element size is 0.25 m (one forth of the smallest dimension of the cavity). The mesh is very fine between the source and the first receiver location. The element size gradually increases towards the boundaries in both directions. For the maximum frequency of interest of about 150 Hz, a time step of 250 μs is chosen for the analysis. The finite element mesh is displayed in Figure 2.

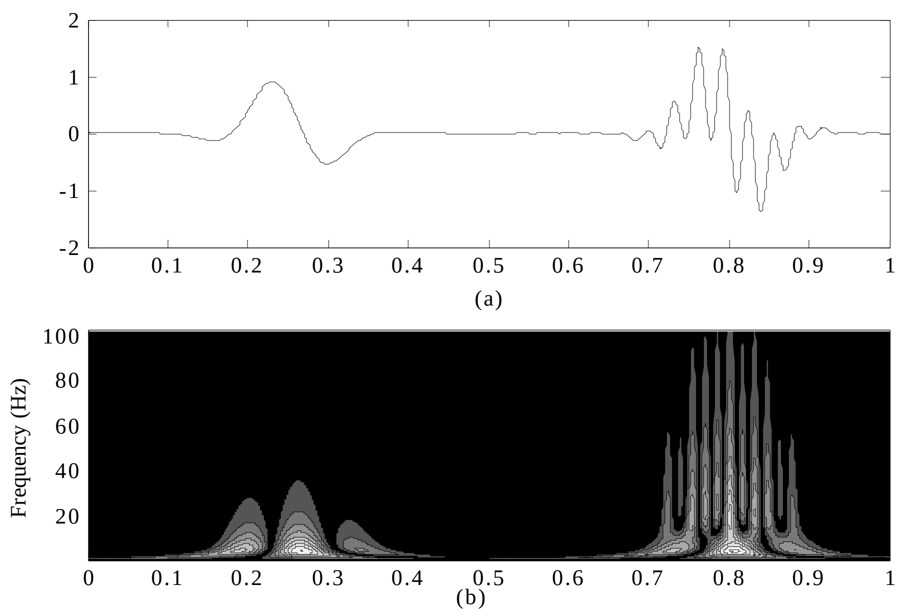

Figure 1- Illustration of Continuous Wavelet Transform (a) Analyzed Synthetic Signal, (b) Signal Gaussian Wavelet Time-Frequency Map.

The characteristics of the different cases of pavement systems considered in this study are listed in Table 1.

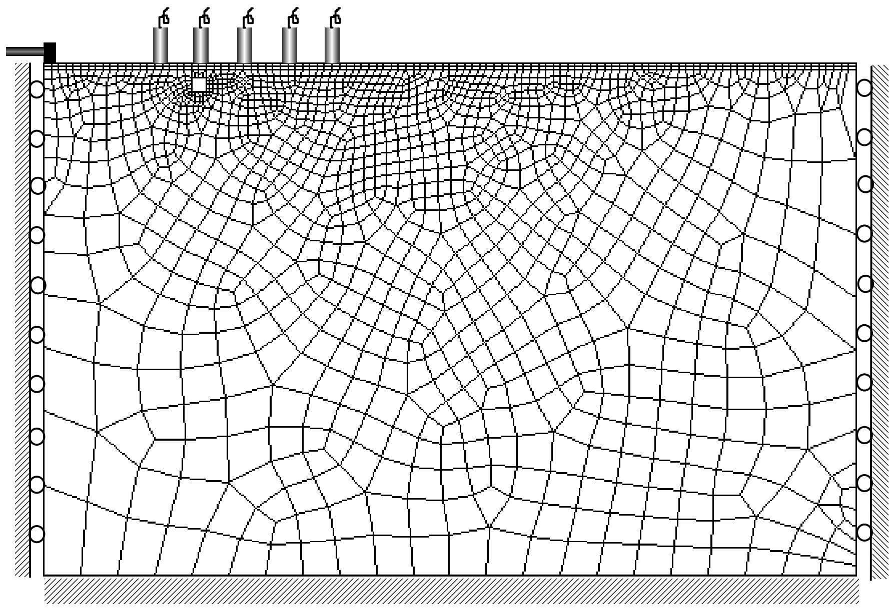

Figure 2- Finite Element Mesh.

Table 1.
Characteristics of different cases.

Case	Pavement Layer	Pavement Thickness (cm)	Cavity	Cavity Width (m)	Cavity Height (m)	Cavity Depth (m)	Cavity Distance (m)
1	X	50	-	-	-	-	-
2	X	25	X	1.0	1.0	1 to 2	10 to 11
3	X	50	X	1.0	1.0	1 to 2	10 to 11
4	X	50	X	2.0	1.0	1 to 2	10 to 12
5	X	50	X	1.0	2.0	1 to 3	10 to 11

WAVELET TRANSFORM ANALYSIS

The seismic impact generates different types of elastic waves in the medium. An abrupt change of impedance on the cavity boundaries results in the reflection of waves towards the impact source. This phenomenon is clearly illustrated in Figure 3, where the normalized time history surface is plotted for Case 2. The position of the cavity is marked in the figure by two dashed lines. It can be observed that packets of waves propagate along straight lines in the receiver location-time plane. The slopes of the lines define the group velocity of the wave packets and can be used to identify the wave packet type. Two Rayleigh waves reflected from the cavity are shown. The Rayleigh waves correspond to the waves reflected from the near and far faces of the cavity. Because of the conversion of waves from one type to another, a number of other reflected wave components are generated close to the cavity. The reflected wave components can be identified only in enlarged plots. Since the surface waves dominate the wave field near the surface, the influence of other types of incident and reflected waves is low, and in most cases may be ignored in the analysis.

The reflected surface waves from the cavity boundaries change the time and frequency characteristics of the surface response. To investigate the effects of subsurface cavities on the near-surface wave patterns, the response at different surface points (receiver locations) for each case is analyzed using Gaussian wavelet transform, and presented in the form of wavelet time frequency maps. These changes have been used to locate and characterize the cavities.

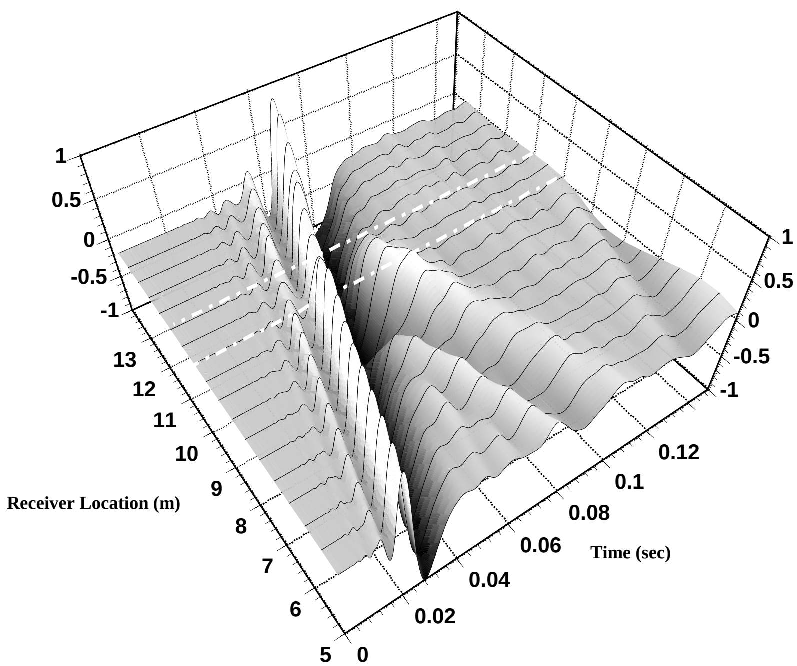

Figure 3- Normalized Time History Surface for Case 2.

A typical surface record and its corresponding Gaussian wavelet time-frequency map is illustrated in Figure 4. It can be observed that the changes in the signal appear as peaks in the wavelet time-frequency maps. The first four peaks (peaks I, II, III and, IV) clearly mark the arrival of different components of incident waves; the last three peaks (peaks V, VI and, VII) correspond to the changes in the signal due to the arrival of reflected waves from the cavity boundaries. On the other hand, the frequency characteristics of each peak demonstrate the frequency distribution of the signal over the duration of the peak. Therefore, wavelet transform provides a localized time-frequency representation of the surface response.

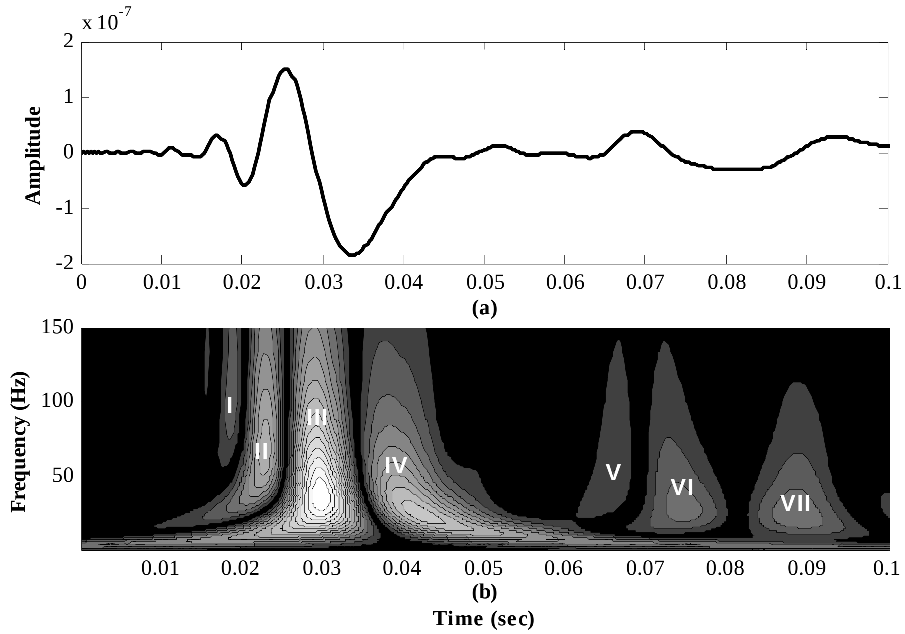

Figure 4- (a) A Typical Surface Record, (b) The Corresponding Wavelet Time-Frequency Map.

To study the effects of cavities, the wavelet time-frequency maps for the response at a distance of 6.0 m (from the source) for all cases are presented in Figures 5 and 6. Peaks I, II, III, and IV in Figure 5(a) clearly mark the arrival of different components of elastic waves generated in the medium, namely, compression, shear and surface waves. Comparing Figures 5(b) and (c) to Figure 5(a) demonstrates the changes in the response due to the presence of the cavity. Although incident wave peaks (I, II, III and, IV) are still present, a new set of peaks (V, VI and, VII) appears in these Figures. These peaks apparently mark the arrival of the reflected waves from the two faces of the cavity. Since the cavity is in the same distance for both cases, the time position of the reflection peaks are almost the same in Figures 5(b) and (c). However, the thicker pavement layer in Case 3 causes a slight shift of the reflection peaks to the left which is a direct consequence of wave traveling in a faster medium. Knowing the surface wave velocity of the medium, the location of the cavity can be estimated from the time position of the reflection peaks. The time difference between the reflection peaks ,as well as their time bandwidths in each case, are controlled by the width the cavity. As expected, is the same for Cases 2 and 3.

The effects of size and shape of the cavity are investigated in Figure 6 where the wavelet time-frequency maps for Cases 4 and 5 are presented. The wider the cavity, the longer the time delay between the arrivals of the reflected waves from its near and far faces. Therefore, the reflection peaks are expected to become wider and better separated. This fact can be easily viewed in Figure 6(a). On the other hand, as the width of the cavity increases, the frequency of the reflection peaks decreases. The decrease in the peak frequency is attributed to a decrease in the natural frequency of the cavity. Therefore, wider cavities cause wider well-separated reflection peaks of relatively lower frequency. Having the surface wave velocity of the medium, the time difference between these two peaks can be easily used to estimate the width of the cavity. An increase in the height of the cavity results in stronger reflections and more pronounced reflection peaks (Figure 6(b)). The reflection peak in this case covers a broader frequency range and is of higher energy. However, having the same width as that of the cavity in Case 2, the time bandwidth of the reflection peaks remains unchanged.

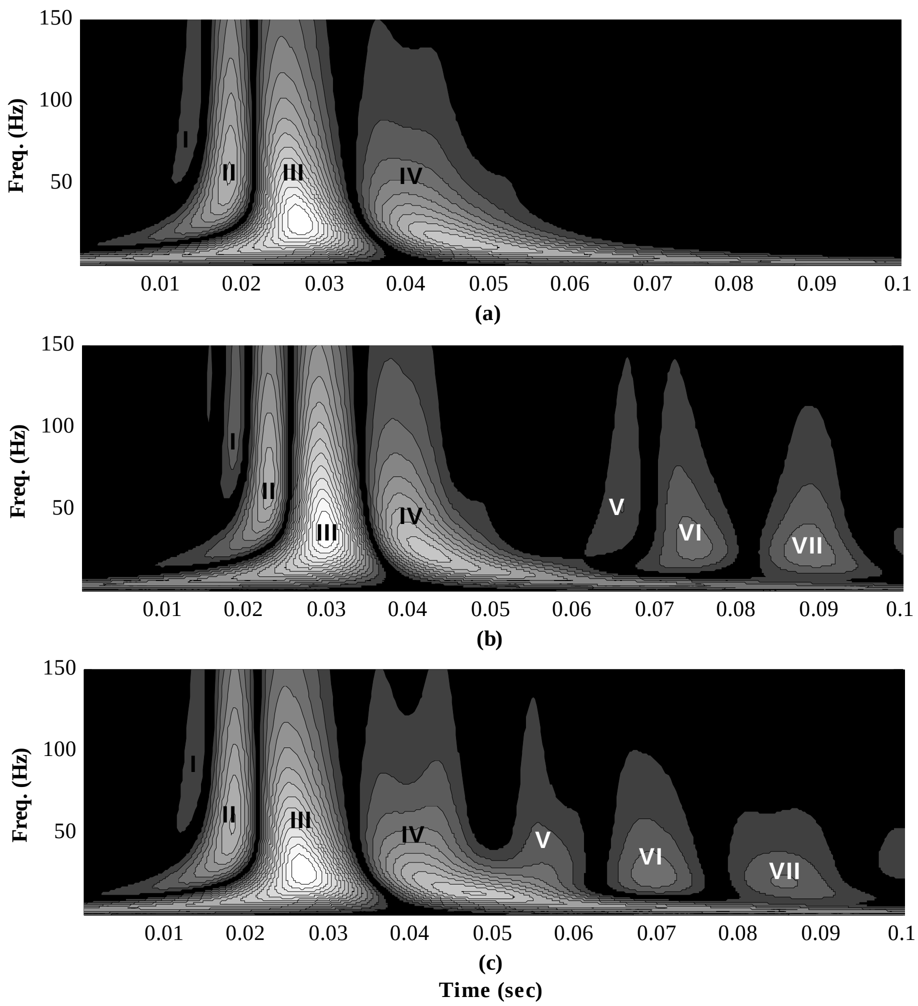

Figure 5- Wavelet Time-Frequency Maps for Response at Distance 6m from the Source for (a) Case 1, (b) Case 2 and, (c) Case 3.

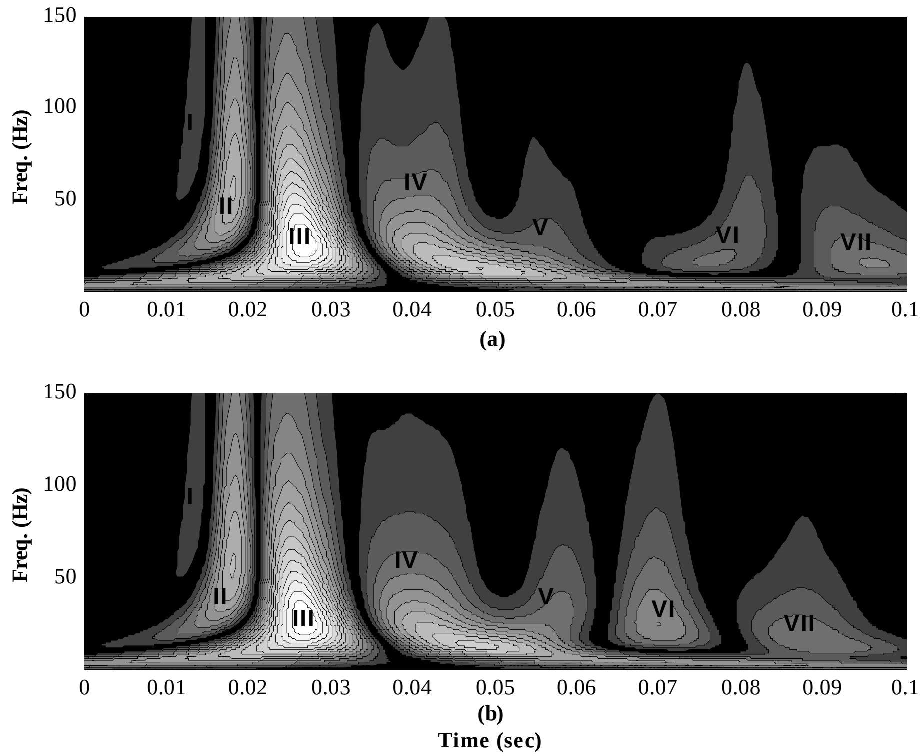

Figure 6- Wavelet Time-Frequency Maps at distance 6m from the Source for (a) Case 4, (b) Case 5.

The results presented in Figures 5 and 6 were the analyses of the surface response for different cases at a single receiver location (at a distance of 6m from the impact source). In practice, analysis of the response at a single surface point would not be generally sufficient. To study the changes in the response at different receiver locations, wavelet time-frequency maps for Cases 2 and 3 at different receiver locations in front of the cavity (5m, 6m, 7m, 8m, 9m and, 10m) are presented in Figures 7 and 8 respectively. As it can be observed, reflections from the cavity boundaries are easily identified for all the receiver locations in front of the cavity. Yet, there is no noticeable signature of the cavity in the wavelet maps at receiver location 10m, where the near face of the cavity is located. Therefore, having the surface response at different directions, the cavity is located along the line where a similar pattern of changes is observed. Also, the location of the cavity can be easily estimated as close to the receiver locations where the reflection peaks vanish.

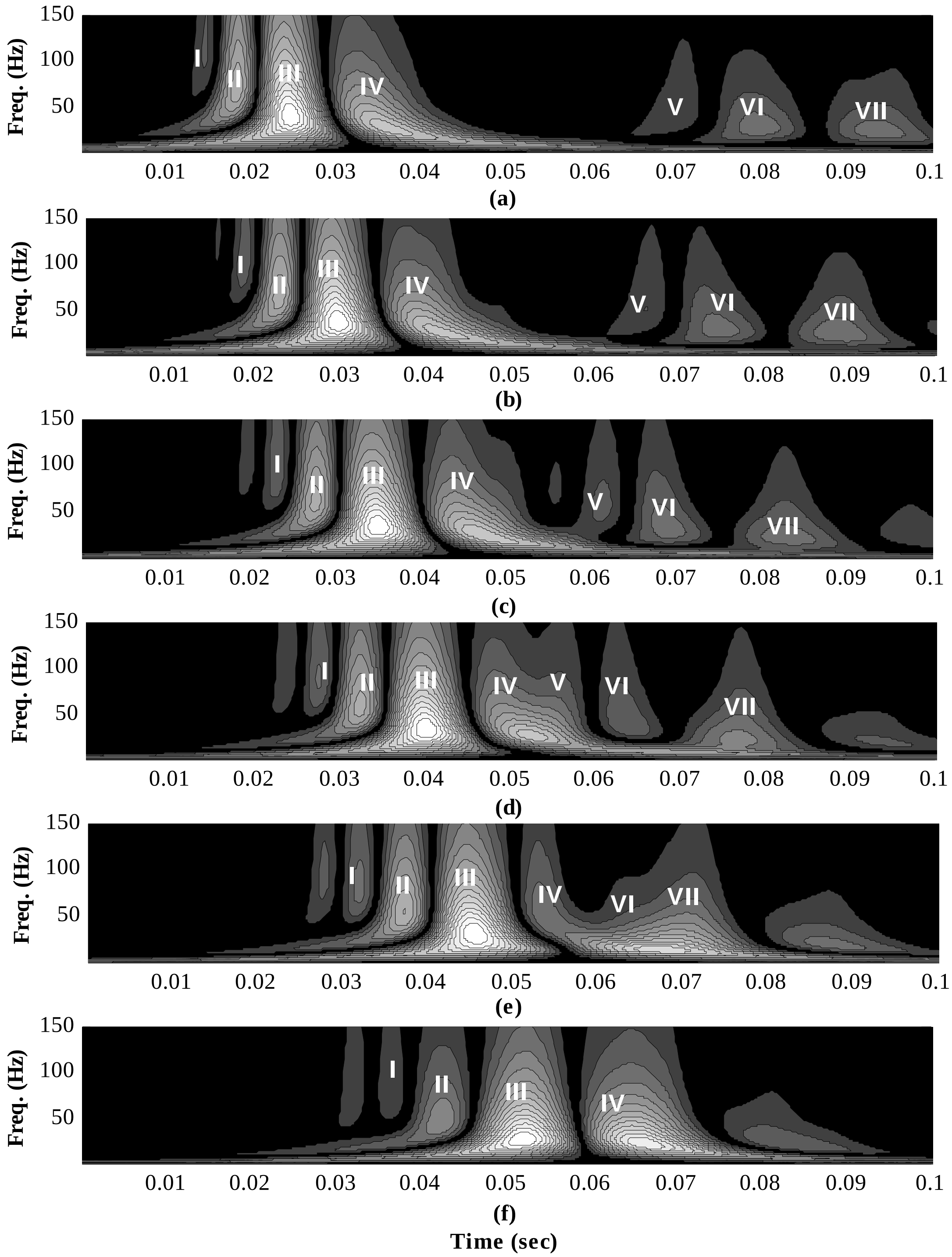

Figure 7- Wavelet Time-Frequency Maps for Case1 at (a) 5m, (b) 6m, (c) 7m, (d) 8m, (e) 9m, (f) 10m from the Impact Source.

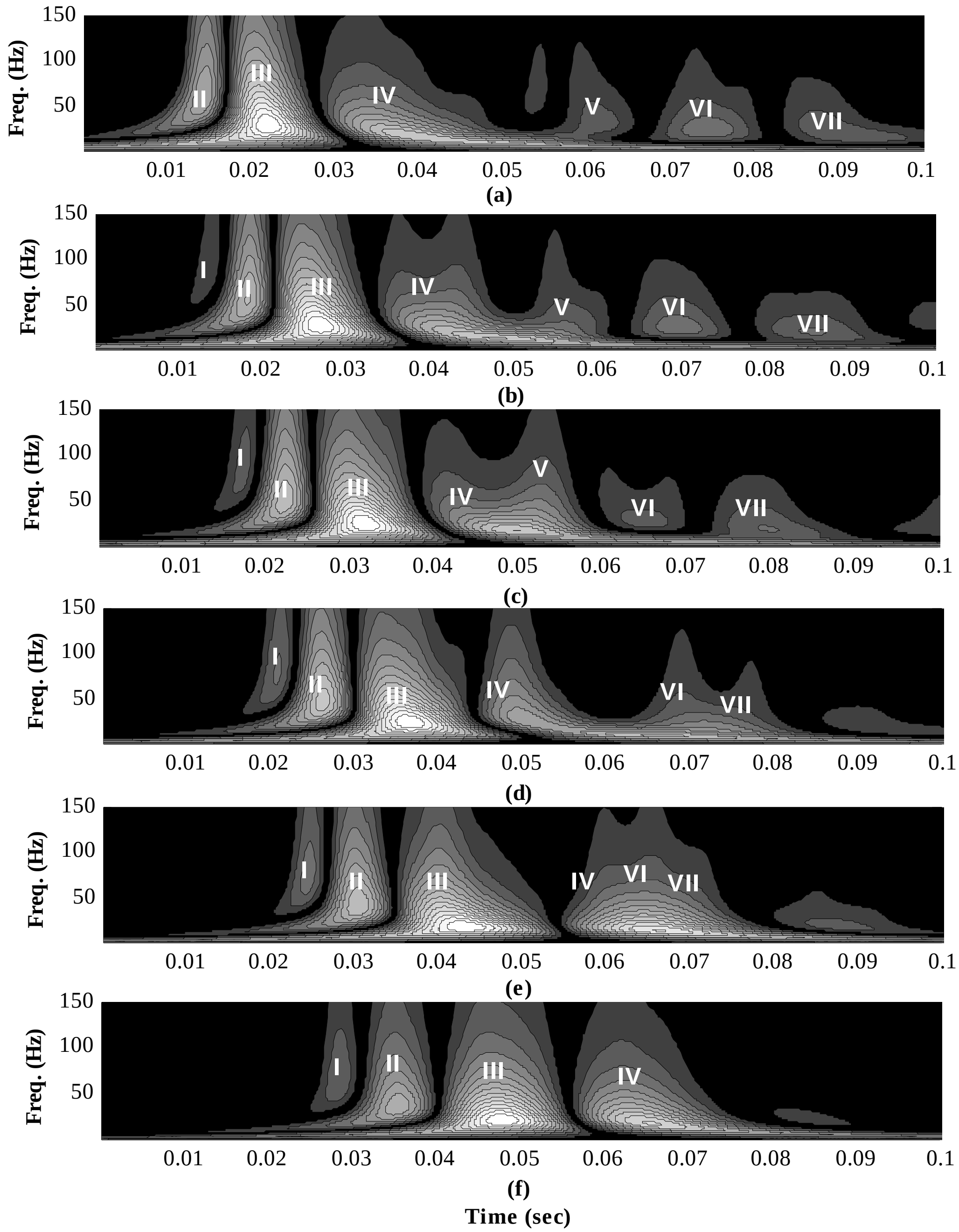

Figure 8- Wavelet Time-Frequency Maps for Case2 at (a) 5m, (b) 6m, (c) 7m, (d) 8m, (e) 9m, (f) 10m from the Impact Source.

The results and observations presented in this paper are quantitatively very similar to those reported by the authors [8,9] for cavity detection in a homogeneous medium. Therefore, it is concluded that a very similar cavity detection scheme can be utilized for location and characterization of the cavity under the airfield thick pavement systems.

CAVITY DETECTION SCHEME

Based on the wavelet analysis results, the following scheme for cavity detection is proposed:

1. Obtain and analyze the surface response for different radial directions, as well as a number of receiver positions along each direction, and present the results in the form of time-frequency maps.

2. Compare the pattern of changes in the time-frequency maps for each direction to those shown in Figures 7 and 8. Choose the direction for which the changes in the maps resemble the most those in the presented pattern. If necessary, obtain the surface response in the selected direction at smaller receiver distances.

3. Approximate the location of the cavity based on the pattern of changes of time-frequency maps. The cavity is located near the receiver position where the reflection peaks vanish.

4. Calculate the distance of the near side of the cavity from the time position of the reflection peak in each time-frequency map (for each receiver position). The accuracy will increase if calculated for different locations and averaged.

5. Calculate the width of the cavity from the time bandwidth of the reflection peak. The accuracy will increase by averaging the time bandwidth for different receiver locations.

6. Determine the shape of the cavity from the time and frequency characteristics of the reflection peak. If the cavity is wide enough, the reflection peak will be recognized by two distinguished hats, a low peak frequency and a narrow frequency bandwidth. The vertical elongation results in peaks of significantly higher energy levels and broader frequency ranges.

7. Cavities with an embedment depth of more than two times their size will be difficult to detect. In general, increasing the depth will result in reflection peaks of lower energy and narrower frequency bandwidths.

CONCLUSION

A new technique for subsurface void detection under the airfield thick pavements using wavelet transforms of the surface seismic response is proposed in this study. The technique is verified numerically using extensive finite element analysis of thick pavement systems. The results were found to be very similar to the findings from the previous numerical and field studies where the same technique was deployed for detection of cavities in a homogeneous medium and under roadway pavement systems. Based on the proposed technique, a step-by-step cavity detection scheme was given. Although the conducted preliminary field tests confirm the results obtained from the numerical studies, the method needs further experimental verification. The potential of using the proposed scheme for detection of cavities under the airport pavements should be evaluated through laboratory and field experiments. This task is the continuation of this ongoing research.

REFERENCES

1. Malvar, L. J., and Cline, G., “Airfield Pavement Void Detection Technology,” Special Publication SP-2081-SHR, Naval Facilities Engineering Service Center, 2000.
2. Cooper, S. S., and Ballard, R. F., “Geophysical Exploration for Cavity Detection in Karst Terrain,” Proceedings of the Symposium on Geotechnical Aspects of Karst Terrains: Exploration, Foundation Design and Performance, and Remedial Measures, ASCE, Geotechnical Special Publications No. 14, New York City, New York, USA, 1988.
3. Belesky, R. M., and Hardy, H. R., “Seismic and Microseismic Methods for Cavity Detection and Stability Monitoring of Near-Surface Voids,” Proceedings of the 27th US Symposium on Rock Mechanics: Key to Energy Production, University of Alabama, Tuscaloosa, Alabama, pp. 248-258, 1986.
4. Nazarian, S., and Stoke II, K. H., “Use of Surface Waves in Pavement Evaluation,” Transportation Research Record 1070, TRB, National Research Council, Washington D. C., pp.132-144, 1986.
5. Al-Shayea, N. A., Woods, R. D., and Gilmore, P., “SASW and GPR to Detect Buried Objects,” Proceedings of the Symposium on the Application of Geophysics to Engineering and Environmental Problems, EEGS, Wheat Ridge, Colorado, pp. 543-560. 1994.
6. Gucunski, N., Ganji, V., and Maher, M., “Effects of Obstacles on Rayleigh Wave Dispersion Obtained from the SASW Test,” Soil Dynamics and Earthquake Engineering, Vol. 15, No. 4, pp.223-231, 1996.
7. Ganji, V., Gucunski, N. and Maher, A., “ Detection of Underground Obstacles by SASW Method: Numerical Aspects,” Journal of Geotechnical and Geoenvironmental Engineering, Vol. 123,No. 3, pp. 212-219, 1997.
8. Shokouhi, P., and Gucunski, N., “Application of wavelet transform in detection of shallow cavities by surface waves,” Symposium on the Application of Geophysics to Engineering and Environmental Problems, EEGS, San Antonio, Texas, 2003.
9. Shokouhi, P., and Gucunski, N., and Maher, A., “ Application of Wavelets in Detection of Cavities under Pavements by Surface Waves,” accepted for publication in Transportation Research Record 1860, TRB, National Research Council, Washington D. C, 2003.
10. Zerwer, A., Cascante, G. and Hutchinson, J., “Parameter Estimation in Finite Element Simulation of Rayleigh Waves,” Journal of Geotechnical & Environmental Engineering, Vol. 128, No. 3, pp. 250-261, 2002.
11. Kaiser, G., *A Friendly Guide to Wavelets*, Birkhauser, Boston, 3-77, 1994.
12. Newland, D. E., “Wavelet Analysis of Vibration, Part I: Theory,” Journal of Vibration and Acoustics, Vol. 116, pp. 409-416, 1994.
13. Walker, J. S., *A primer on wavelets and their scientific applications*, CRC Press, 1999.